Imaging the partonic structure of the nucleon

Barbara Pasquini

Dipartimento di Fisica, Università degli Studi di Pavia, I-27100 Pavia, Italy
Istituto Nazionale di Fisica Nucleare, Sezione di Pavia, I-27100 Pavia, Italy
barbara.pasquini@unipv.it

Abstract. We discuss the main properties of different types of parton distribution functions, which provide complementary multidimensional images of the partonic structure of the nucleon. These distributions are the generalized parton distributions, the transverse-momentum dependent parton distributions and the Wigner distributions. They have attracted increasing attention in the last years as they represent new tools to study how the composite structure of the proton results from the underlying quark-gluon dynamics.

Keywords: generalized parton distributions; transverse-momentum dependent parton distributions; Wigner distributions

1 Introduction

For a long time, the parton distributions have been explored in collinear processes such as fully inclusive deep inelastic scattering processes. This corresponds to a one-dimensional imaging of the proton as a set of partons moving collinearly with the direction of motion of the parent hadron, identified as the longitudinal direction. Recently, it has become clear that exclusive processes or semi-inclusive deep inelastic processes open the way to study the partonic structure of hadrons in more dimensions, using, respectively, generalized parton distributions (GPDs) and transverse-momentum dependent parton distributions (TMDs). GPDs can be used to map the partons in a mixed space of transverse spatial coordinates and longitudinal momentum. TMDs generalize the concept of collinear parton distributions by including also the dependence on the transverse momentum of the partons. GPDs and TMDs are truly independent functions, but can be seen as different projections of a larger class of distributions, known as generalized transverse-momentum dependent parton distributions (GTMDs). GTMDs have a direct connection with the Wigner functions, which represent the quantum mechanical analogues of the classical phase-space distributions. In the following sections, we will discuss key features of these distributions and our present understanding from available experimental data.

2 Generalized parton distributions

Exclusive electroproduction of a real photon or a meson off a nucleon target at high momentum transfer is theoretically the cleanest way to access GPDs. Owing

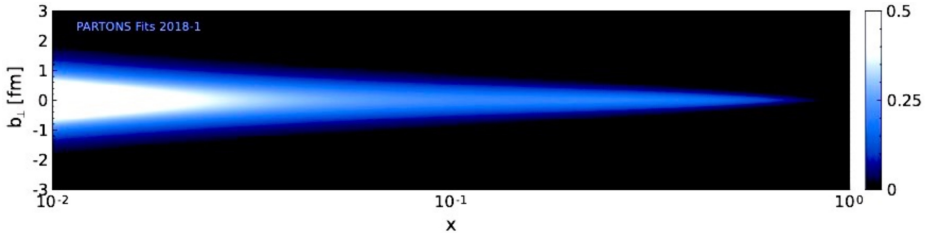

Fig. 1. The transverse position $b_\perp$ of up quarks in an unpolarized proton as a function of the longitudinal momentum fraction x. (Adapted from [59]).

to the factorization property of QCD, these processes give access to different flavor combination of GPDs and are complementary to disentangle the various GPDs (see, e.g., Refs. [46, 26] for recent reviews of the GPD phenomenology). GPDs depend on three variables (considering the dependence on the factorization scale Q^2 to be known): x, that is the fraction of average longitudinal momentum of the active quark, referred to the average target momentum; the skewness variable ξ and t, that are, respectively, the fraction of longitudinal momentum and four-momentum transferred to the hadron target. However, one does not have direct access to this multidimensional structure, since the dependence on the three variables enters observables in nontrivial convolution with coefficient functions. Therefore, fits of GPDs require educated assumptions for the choice of the fitting functions such to incorporate the known theoretical constraints of GPDs, i.e. polinomiality, sum rules, and positivity (see, e.g., Refs. [30, 21, 38, 9, 13, 31] for a detailed preface to the GPD formalism and properties). Fits existing in the present literature are reasonably successful and it looks like there are no major problems with the theoretical framework.

Impact parameter distributions can be reconstructed by taking a Fourier transform of the GPDs in the variable t at $\xi = 0$. These distributions represent densities of partons with a given fraction of x as function of the position $\mathbf{b}_\perp$ from the centre of momentum of the nucleon in the plane perpendicular to the longitudinal direction [16]. A first attempt to obtain this information directly from photon electroproduction measurements was illustrated in Refs. [23, 22], using a model-dependent extrapolation to the point $\xi = 0$ that is not accessible experimentally. Recently, dispersion relation techniques have been used in Ref. [59] to constraint the GPDs at $\xi = 0$ from data. Both these analysis confirm that the width of the impact-parameter distribution for unpolarized quarks in unpolarized protons has a vey peaked transverse profile in the limit of $x \to 1$, as shown in Fig 1. This behaviour is expected, since, in this limit, the active quark is always very close to the transverse center of momentum [16, 61].

The GPDs can also be viewed as the generating functions for the form factors of the twist-two operators governing the interaction mechanisms of hard processes in the deep inelastic regime. The most peculiar example are the form factors of the energy momentum tensor (EMT), which can be studied indirectly

looking at moments of the GPDs. This is a unique and practical opportunity to access through electromagnetic processes the EMT form factors, which are canonically probed through gravity. We have four independent EMT form factors for the separate quark and gluon contribution, which reduce to three for the sum of quark and gluon terms due to the conservation of the EMT [66]. They are usually referred as $A(t)$, $J(t)$ and $D(t)$. At $t = 0$, the corresponding "charges" for quarks and gluons give, respectively, the fraction of nucleon momentum carried by the partons, the Ji's relation [41] for the quark and gluon contribution to the total angular momentum of the nucleon, and the D-term which is sometimes referred as the "last unknown global property" [66].

The physical content of the information encoded in the EMT form factors is revealed in the so-called Breit frame [65, 66] and has been recently discussed in other frames in Refs. [56, 48]. Working in the Breit frame, the D-term form factor can be related to the spatial distribution of shear forces $s(r)$ and pressure $p(r)$ as

$$p(r) = \frac{1}{3}\int \frac{\mathrm{d}^3\mathbf{\Delta}}{2m(2\pi)^3} e^{-i\mathbf{\Delta}\cdot\mathbf{r}} P_0(\cos\theta)\,[tD(t)]\,, \tag{1}$$

$$s(r) = \frac{3}{4}\int \frac{\mathrm{d}^3\mathbf{\Delta}}{2m(2\pi)^3} e^{-i\mathbf{\Delta}\cdot\mathbf{r}} P_2(\cos\theta)\,[tD(t)]\,, \tag{2}$$

where $t = \mathbf{\Delta}^2$. The relation for the shear forces holds also for quark and gluon separately, while it is defined only for the total system in the case of the pressure. Thanks to Eqs. (1) and (2), the form factor $D(t)$ provides the key to introduce mechanical properties of the nucleon and reflects the internal dynamics of the system through the distribution of forces. Requiring that for the mechanical stability of the system the corresponding force must be directed outwards, one expects the local criterion $2s(r) + p(r) > 0$, which implies that the D-term for any stable system must be negative, $D < 0$, as confirmed in models [43, 29, 20], calculations from dispersion relations [63] and lattice QCD [33] for the nucleon. Another consequence of the EMT conservation is the von Laue condition, which shows how the internal forces balance inside a composed particle, i.e.,

$$\int_0^\infty p(r) r^2 \mathrm{d}r = 0. \tag{3}$$

This relation implies that the pressure must have at least one node. In all model studies so far it was found that the pressure is positive in the inner region, and negative in the outer region, with the positive sign meaning repulsion towards outside and the negative sign meaning attraction directed towards inside. Recently, an analysis of the published JLab data measured at 6 GeV [28, 44] lead to experimental information on the quark contribution to the D-term form factor [19], as shown in Fig. 2 (squared in the left panel, referring to a scale of $\mu^2 = 1.5$ GeV^2), in comparison with the KM15 fit [47] and calculations from dispersion relations [63] and lattice QCD [33] (all to the scale of 4 GeV^2) and scale independent results from the bag [43], chiral quark soliton [29] and Skyrme [20] models. The D-term parameters fitted to the JLab data, with the assumption of

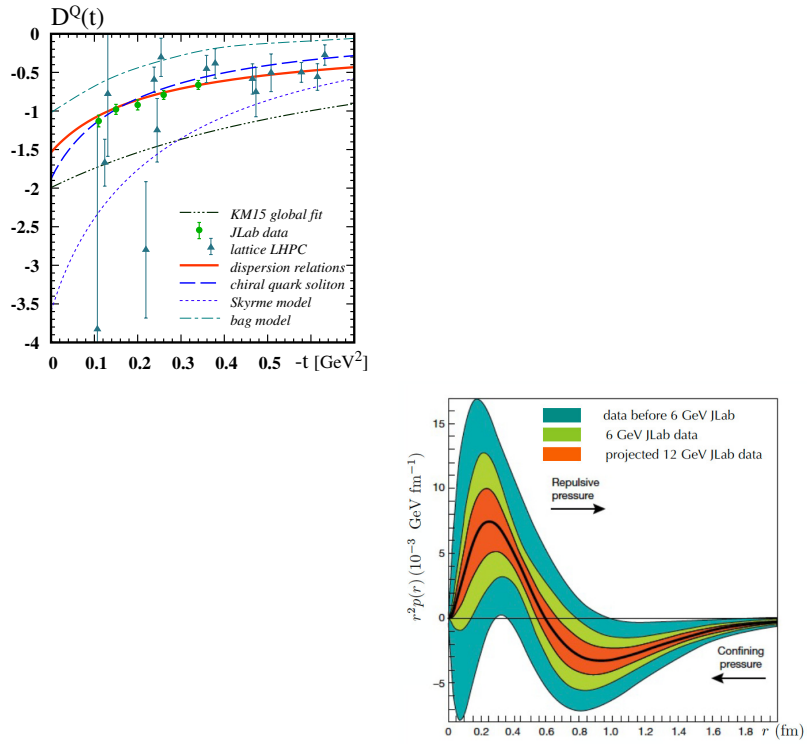

Fig. 2. Left panel (adapted from [66]): The $D^Q(t)$ form factor from the JLab analysis [19], in comparison with the KM15 fit [47] and calculations from dispersion relations [63] and lattice QCD [33], and results from the bag [43], chiral quark soliton [29] and Skyrme [20] model. Right panel (adapted from [19]): quark contribution to the pressure distributions $r^2p(r)$ as function of the radial distance r from the centre of the proton.

a negligible gluon contribution, were used to plot the radial pressure distribution shown by the black solid curve in the right panel of Fig. 2. The corresponding estimated uncertainties are displayed as the light-green shaded area. The blue area represents the uncertainties from all the data that were available before the 6-GeV experiment, and the red shaded area shows projected results from future JLab experiments at 12 GeV. Within the uncertainties of the analysis, the distribution satisfies the stability condition (3), with a zero crossing near $r = 0.6$ fm separating the inner region of a positive repulsive distribution from the outer region with a negative pressure responsible for the binding.

3 Transverse-momentum dependent parton distributions

In order to be sensitive to intrinsic transverse parton momenta it is necessary to measure transverse momenta of the produced hadrons in the final state, e.g., in processes like semi-inclusive lepton-nucleon deep inelastic scattering (SIDIS), hadron production in e^+e^- annihilation or Drell-Yan (DY) processes in hadron-hadron collisions. In all these cases, factorization has been proved at leading twist enabling to access information on TMDs as well as on fragmentation functions (FFs), which describe the hadronization process of the hit quark decaying into the detected hadrons. The study of factorization and evolution properties of TMDs and FFs has rapidly evolved in the last years thanks to the contribution of several groups (see, e.g., the review in Ref. [67] and references therein). While DY and e^+e^- annihilation processes provide independent information on either TMDs or FFs, the SIDIS cross section involves the convolution of one TMD and one FF. Therefore, for a clean extraction of TMDs it is essential to have an independent and unbiased knowledge of FFs. At present, the challenge of the phenomenological extractions is to develop a consistent procedure to analyze all three kind of processes for a simultaneous fit of TMDs and FFs (for a recent review on the phenomenology of TMD see, e.g., Ref. [14] and for a review on TMD and FF measurements see, respectively, Refs. [4] and [27]).

At leading twist, there are eight independent TMDs, three of them surviving when integrated over the transverse momentum and giving rise to the familiar parton density, helicity and transversity distributions. These three TMDs involve matrix elements which are all diagonal in the orbital angular momentum (OAM), but probe different transverse momentum and helicity correlations of the quarks inside the nucleon. Viceversa, the other TMDs vanish without the contribution of quark OAM and contain non-trivial information on the spin-spin and spin-orbit correlations of the partons and nucleon. The OAM content of the different quark TMDs becomes evident when using the representation of TMDs in terms of overlap of light-front wave functions that are eigenstates of the OAM operator [62, 12, 64]. However, we still do not have a direct and rigorous relation between TMDs and OAM, such, for example, in the case of the Ji's relation for GPDs. A relation between OAM and the so called pretzelosity TMD has been suggested [70, 5], but this is valid only within a particular class of models [51, 49] and it is not a rigorous prediction of QCD.

In the following, I will focus on the unpolarized TMD $f_1(x, k_\perp)$ and the Sivers function $f_{1T}^\perp(x, k_\perp)$, which have seen recently a considerable work from the phenomenological point of view. The unpolarized TMD is present in all measurements to construct the spin asymmetries which give access to the polarized TMDs, and therefore represents a fundamental building block. Several extractions of the unpolarized TMD exist in literature (see, e.g., Ref. [14] and references therein). Among them, the recent work by Scimemi and Vladimirov [69] reached the highest currently available level of perturbative accuracy, but it takes into account a limited number of experimental points, coming from DY and Z production. On the other side, the extraction in Ref. [7] applies the TMD evolution at one order lower, but it includes the largest set of data points available from

experiments of different kinds, i.e. SIDIS, DY and Z production, providing an important test for the universality property of TMDs. The present extractions of f_1 give indications that the width of the TMDs at low scales, 1-2 GeV, is around $300 - 500$ MeV and increases to more than 1 GeV at the Z mass, due to TMD evolution. Data indicate also that the width is probably increasing as x decreases and there is room for a flavor dependence, even though also a flavor-independent scenario is not ruled out. There are still important questions that need to be answered with more precision in future analyses [6], also thanks to the availability of new data. For example, we aim to reduce the uncertainties and eventual bias in the choice of the functional form adopted as input in the fit as well as in the prescription to deal with the non-perturbative part of the TMD evolution. The x dependence along with the flavor dependence are practically unknown. Calculations in different models [62, 5, 18, 68] and on lattice [60] indicate that the dependence of the transverse-momentum distributions on the quark polarisation and flavor may be significant at low scale, although it may be reduced under TMD evolution. A thorough study in these directions is driving the upgrades of several existing facilities (JLab, COMPASS and RHIC), and plays an important role also in the design and construction of new facilities worldwide (EIC, FAIR, NICA and JPARC).

The Sivers function describes the difference between the probability to find a quark with longitudinal momentum fraction x and transverse momentum $\mathbf{k}_\perp$ inside a hadron polarised transversely to its momentum direction, and the one where the polarisation points in the opposite direction. As such it encodes the correlation between the partonic intrinsic motion and the transverse spin of the nucleon, and it generates a dipole deformation in momentum space, as shown in Fig. 3 for the density distribution in the transverse momentum space at $x = 0.1$ of unpolarized up and down quarks in a nucleon transversely polarized in the $+y$ direction. The Sivers function has been phenomenologically extracted by several groups, mainly from analysing the azimuthal distributions of single hadrons in SIDIS (see, e.g., the review of the different works in Ref. [14]). The existence of the Sivers function as well as of the homolog Boer-Mulders function, describing transversely polarized quarks in an unpolarized nucleon, is ultimately related to initial-state and final-state collinear gluon interactions, which are summed into two different gauge links. This difference in the gauge link leads to a modified universality properties of the Sivers and Boer-Mulders functions, consisting in a sign flip in going from SIDIS to DY processes. First experimental evidences of this sign change of the Sivers function come from the transverse spin asymmetries measured at RHIC in transversely polarized proton-proton collision [2] and the pion-induced DY measurements at COMPASS [3].

4 Wigner distributions

The concept of Wigner distributions in QCD for quarks and gluons was first explored in Refs. [42, 8]. In these works, the standard three-dimensional Fourier transform in the Breit frame was used, leading to six-dimensional Wigner dis-

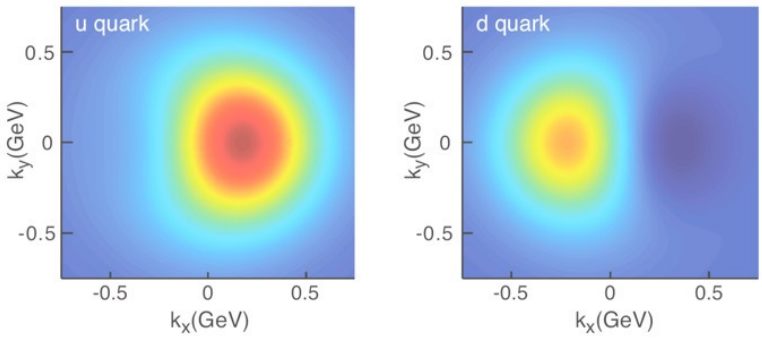

Fig. 3. Distributions in the transverse-momentum plane, at fixed $x = 0.1$, of unpolarized up and down quarks inside a proton transversely polarized in the $+y$ direction, as described by the Sivers function. The deep red (blue) indicates large negative (positive) values for the Sivers function. (Adapted from [1]).

tributions (three position and three momentum coordinates), which are valid only for infinitely massive target in order to get rid of relativistic corrections. A five-dimensional phase-space distribution free of relativistic corrections was introduced within the light-front formalism in Ref. [50]. In this case, the Wigner distributions appear to be the Fourier transform of GTMDs [57, 58, 52, 24], which reduce in particular limits to GPDs and TMDs. However, the Wigner distributions contain richer physics than TMDs and GPDs combined, as they carry information about the correlations between the quark momentum $(x, \mathbf{k}_\perp)$ and transverse space position $\mathbf{b}_\perp$, which cannot be accessed by separately studying TMDs or GPDs. Because of the uncertainty principle which prevents knowing simultaneously the position and momentum of a quantum-mechanical system, these phase-space distributions do not have a simple probabilistic interpretation. For this reason, they are often called quasi distributions, and only in the classical limit they become positive definite. Nonetheless, the physics of phase-space distributions is very rich and one can try to select certain situations where a semiclassical interpretation is still possible. Currently, the best hope to access the GTMDs is in the low-x regime for the gluon contribution [32, 36, 35, 40, 10, 15], while a single process has been identified sofar for the quark sector [11].

At leading twist, there are 32 quark phase-space distributions, half of them being associated to naive T-odd GTMDs and hence encoding initial and/or final-state interactions. A detailed study of these distributions has been presented in Refs. [50, 53]. All the contributions can be understood as encoding all the possible correlations between target and quark angular momenta, see Table 1. In particular, the function ρ_{LU} for unpolarized quarks in a longitudinally polarized nucleon has attracted considerable attention because it gives direct access to the quark OAM. One has just to take the phase-space average of the classical expression $(\mathbf{b}_\perp \times \mathbf{k}_\perp)$ of the OAM as if the Wigner distributions were classical

distributions [50, 55], i.e.

$$L_z^{q,g} = \int \mathrm{d}x \mathrm{d}^2\mathbf{b}_\perp \mathrm{d}^2\mathbf{k}_\perp^2 (\mathbf{b}\times\mathbf{k}_\perp)\rho_{LU}^{q,g}(x,\mathbf{b}_\perp,\mathbf{k}_\perp;\mathcal{W}), \tag{4}$$

$$= \int \mathrm{d}^2\mathbf{b}_\perp \mathbf{b}_\perp \times \langle \mathbf{k}_\perp\rangle^{q,g}, \tag{5}$$

where $\langle \mathbf{k}_\perp\rangle^{q,g}$ is the distribution in impact-parameter space of the quark/gluon mean transverse momentum, i.e.

$$\langle \mathbf{k}_\perp\rangle^{q,g} = \int \mathrm{d}x \mathrm{d}^2\mathbf{k}_\perp \mathbf{k}_\perp \rho_{LU}^{q,g}(x,\mathbf{b}_\perp,\mathbf{k}_\perp;\mathcal{W}). \tag{6}$$

In Eq. (4), the shape of the Wilson line $\mathcal{W}$ determines the type of OAM [34, 17]. For a staple-like Wilson line, like e.g. the one involved in the description of SIDIS scattering and DY processes, Eq. (4) leads to the canonical quark/gluon OAM, corresponding to the Jaffe-Manohar definition [37], irrespective of whether the staple is future or past-pointing. For a straight Wilson line, it leads to the kinetic quark OAM, corresponding to the Ji's definition [41], and to the Ji-Xiong-Yuan [39] definition of the gauge-invariant gluon OAM. Under a Fourier transform, the phase-space distribution is related to the GTMD $F_{1,4}$ [50, 34, 45], providing a relation between the OAM and GTMDs that gives access to the so far elusive canonical OAM in lattice QCD [25]. As an example, in Fig. 4 we show the distribution of the quark mean transverse momentum obtained within a light-front constituent quark model [55, 54]. We clearly see that in a longitudinally polarized nucleon, the quarks have on average nonzero OAM. The u quarks tend to orbit anti-clockwise inside the nucleon, corresponding to $L_z^u > 0$ since the proton is represented with its spin pointing out of the figure. For the d quarks, we see two regions. In the central region of the nucleon, $b_\perp < 0.3$ fm, the d quarks tend to orbit anti-clockwise like the u quarks. In the peripheral region, $b_\perp > 0.3$ fm, the d quarks tend to orbit clockwise. The mean transverse momentum $\langle \mathbf{k}_\perp\rangle^q$ is always orthogonal to the impact-parameter vector $\mathbf{b}_\perp$. In principle, there can also be a radial component, representing the effect of initial and final state interactions. Such interactions being absent in the model, we do not see any radial contribution.

Table 1. Correlations between target polarization $(S_L, \boldsymbol{S}_T)$, quark polarization $(S_L^q, \boldsymbol{S}_T^q)$ and quark OAM $(\ell_L^q, \boldsymbol{\ell}_T^q)$ encoded in the various phase-space distributions ρ_X. U, L, T stand, respectively, for unpolarized, and longitudinal and transverse polarizations.

ρ_X	U	L	T_x	T_y
U	$\langle 1\rangle$	$\langle S_L^q \ell_L^q\rangle$	$\langle S_x^q \ell_x^q\rangle$	$\langle S_y^q \ell_y^q\rangle$
L	$\langle S_L \ell_L^q\rangle$	$\langle S_L S_L^q\rangle$	$\langle S_L \ell_L^q S_x^q \ell_x^q\rangle$	$\langle S_L \ell_L^q S_y^q \ell_y^q\rangle$
T_x	$\langle S_x \ell_x^q\rangle$	$\langle S_x \ell_x^q S_L^q \ell_L^q\rangle$	$\langle S_x S_x^q\rangle$	$\langle S_x \ell_x^q S_y^q \ell_y^q\rangle$
T_y	$\langle S_y \ell_y^q\rangle$	$\langle S_y \ell_y^q S_L^q \ell_L^q\rangle$	$\langle S_y \ell_y^q S_x^q \ell_x^q\rangle$	$\langle S_y S_y^q\rangle$

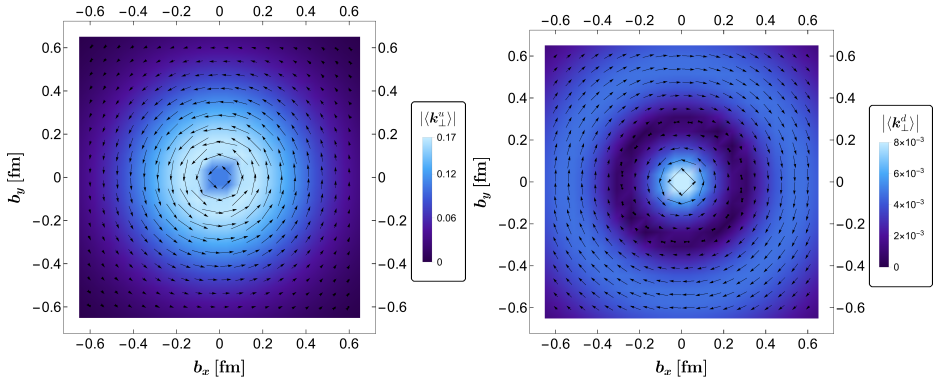

Fig. 4. Distributions in impact parameter space of the mean transverse momentum $< \mathbf{k}_\perp^q >$ [fm^{-3}] of unpolarized quarks in a longitudinally polarized nucleon. The nucleon polarization is pointing out of the plane, while the arrows show the size and direction of the mean transverse momentum of the quarks. The left (right) panel shows the results for u (d) quarks. (Adapted from [55]).

Acknowledgement

This work is partially supported by the European Research Council (ERC) under the European Union's Horizon 2020 research and innovation programme (grant agreement No. 647981, 3DSPIN).

References

1. Accardi, A., et al.: Eur. Phys. J. **A52**(9), 268 (2016)
2. Adamczyk, L., et al.: Phys. Rev. Lett. **116**(13), 132301 (2016)
3. Aghasyan, M., et al.: Phys. Rev. Lett. **119**(11), 112002 (2017)
4. Avakian, H., Bressan, A., Contalbrigo, M.: Eur. Phys. J. **A52**(6), 150 (2016). [Erratum: Eur. Phys. J.A52,no.6,165(2016)]
5. Avakian, H., Efremov, A.V., Schweitzer, P., Yuan, F.: Phys. Rev. **D81**, 074035 (2010)
6. Bacchetta, A.: Eur. Phys. J. **A52**(6), 163 (2016)
7. Bacchetta, A., Delcarro, F., Pisano, C., Radici, M., Signori, A.: JHEP **06**, 081 (2017)
8. Belitsky, A.V., Ji, X.d., Yuan, F.: Phys. Rev. **D69**, 074014 (2004)
9. Belitsky, A.V., Radyushkin, A.V.: Phys. Rept. **418**, 1 (2005)
10. Bhattacharya, S., Metz, A., Ojha, V.K., Tsai, J.Y., Zhou, J.: arXiv:1802.10550 [hep-ph]
11. Bhattacharya, S., Metz, A., Zhou, J.: Phys. Lett. **B771**, 396 (2017)
12. Boffi, S., Efremov, A.V., Pasquini, B., Schweitzer, P.: Phys. Rev. **D79**, 094012 (2009)
13. Boffi, S., Pasquini, B.: Riv. Nuovo Cim. **30**, 387 (2007)
14. Boglione, M., Prokudin, A.: Eur. Phys. J. **A52**(6), 154 (2016)

15. Boussarie, R., Hatta, Y., Xiao, B.W., Yuan, F.: Phys. Rev. **D98**(7), 074015 (2018)
16. Burkardt, M.: Int. J. Mod. Phys. **A18**, 173 (2003)
17. Burkardt, M.: Phys. Rev. **D88**(1), 014014 (2013)
18. Burkardt, M., Pasquini, B.: Eur. Phys. J. **A52**(6), 161 (2016)
19. Burkert, V.D., Elouadrhiri, L., Girod, F.X.: Nature **557**(7705), 396 (2018)
20. Cebulla, C., Goeke, K., Ossmann, J., Schweitzer, P.: Nucl. Phys. **A794**, 87 (2007)
21. Diehl, M.: Phys. Rept. **388**, 41 (2003)
22. Dupré, R., Guidal, M., Niccolai, S., Vanderhaeghen, M.: Eur. Phys. J. **A53**(8), 171 (2017)
23. Dupré, R., Guidal, M., Vanderhaeghen, M.: Phys. Rev. **D95**(1), 011501 (2017)
24. Echevarria, M.G., Idilbi, A., Kanazawa, K., Lorcé, C., Metz, A., Pasquini, B., Schlegel, M.: Phys. Lett. **B759**, 336 (2016)
25. Engelhardt, M.: Phys. Rev. **D95**(9), 094505 (2017)
26. Favart, L., Guidal, M., Horn, T., Kroll, P.: Eur. Phys. J. **A52**(6), 158 (2016)
27. Garzia, I., Giordano, F.: Eur. Phys. J. **A52**(6), 152 (2016)
28. Girod, F.X., et al.: Phys. Rev. Lett. **100**, 162002 (2008)
29. Goeke, K., Grabis, J., Ossmann, J., Polyakov, M.V., Schweitzer, P., Silva, A., Urbano, D.: Phys. Rev. **D75**, 094021 (2007)
30. Goeke, K., Polyakov, M.V., Vanderhaeghen, M.: Prog. Part. Nucl. Phys. **47**, 401 (2001)
31. Guidal, M., Moutarde, H., Vanderhaeghen, M.: Rept. Prog. Phys. **76**, 066202 (2013)
32. Hagiwara, Y., Hatta, Y., Pasechnik, R., Tasevsky, M., Teryaev, O.: Phys. Rev. **D96**(3), 034009 (2017)
33. Hagler, P., et al.: Phys. Rev. **D77**, 094502 (2008)
34. Hatta, Y.: Phys. Lett. **B708**, 186 (2012)
35. Hatta, Y., Nakagawa, Y., Yuan, F., Zhao, Y., Xiao, B.: Phys. Rev. **D95**(11), 114032 (2017)
36. Hatta, Y., Xiao, B.W., Yuan, F.: Phys. Rev. Lett. **116**(20), 202301 (2016)
37. Jaffe, R.L., Manohar, A.: Nucl. Phys. **B337**, 509 (1990)
38. Ji, X.: Ann. Rev. Nucl. Part. Sci. **54**, 413 (2004)
39. Ji, X., Xiong, X., Yuan, F.: Phys. Rev. **D88**(1), 014041 (2013)
40. Ji, X., Yuan, F., Zhao, Y.: Phys. Rev. Lett. **118**(19), 192004 (2017)
41. Ji, X.D.: Phys. Rev. Lett. **78**, 610 (1997)
42. Ji, X.d.: Phys. Rev. Lett. **91**, 062001 (2003)
43. Ji, X.D., Melnitchouk, W., Song, X.: Phys. Rev. **D56**, 5511 (1997)
44. Jo, H.S., et al.: Phys. Rev. Lett. **115**(21), 212003 (2015)
45. Kanazawa, K., Lorcé, C., Metz, A., Pasquini, B., Schlegel, M.: Phys. Rev. **D90**(1), 014028 (2014)
46. Kumericki, K., Liuti, S., Moutarde, H.: Eur. Phys. J. **A52**(6), 157 (2016)
47. Kumericki, K., Müller, D.: EPJ Web Conf. **112**, 01012 (2016)
48. Lorcé, C., Mantovani, L., Pasquini, B.: Phys. Lett. **B776**, 38 (2018)
49. Lorcé, C., Pasquini, B.: Phys. Rev. **D84**, 034039 (2011)
50. Lorcé, C., Pasquini, B.: Phys. Rev. **D84**, 014015 (2011)
51. Lorcé, C., Pasquini, B.: Phys. Lett. **B710**, 486 (2012)
52. Lorcé, C., Pasquini, B.: JHEP **09**, 138 (2013)
53. Lorcé, C., Pasquini, B.: Phys. Rev. **D93**(3), 034040 (2016)
54. Lorcé, C., Pasquini, B., Vanderhaeghen, M.: JHEP **05**, 041 (2011)
55. Lorcé, C., Pasquini, B., Xiong, X., Yuan, F.: Phys. Rev. **D85**, 114006 (2012)
56. Lorc, C., Moutarde, H., Trawiski, A.P.: Eur. Phys. J. **C79**(1), 89 (2019)

57. Meissner, S., Metz, A., Schlegel, M.: JHEP **08**, 056 (2009)
58. Meissner, S., Metz, A., Schlegel, M., Goeke, K.: JHEP **08**, 038 (2008)
59. Moutarde, H., Sznajder, P., Wagner, J.: Eur. Phys. J. **C78**(11), 890 (2018)
60. Musch, B.U., Hagler, P., Negele, J.W., Schafer, A.: Phys. Rev. **D83**, 094507 (2011)
61. Pasquini, B., Boffi, S.: Phys. Lett. **B653**, 23 (2007)
62. Pasquini, B., Cazzaniga, S., Boffi, S.: Phys. Rev. **D78**, 034025 (2008)
63. Pasquini, B., Polyakov, M.V., Vanderhaeghen, M.: Phys. Lett. **B739**, 133 (2014)
64. Pasquini, B., Yuan, F.: Phys. Rev. **D81**, 114013 (2010)
65. Polyakov, M.V.: Phys. Lett. **B555**, 57 (2003)
66. Polyakov, M.V., Schweitzer, P.: Int. J. Mod. Phys. **A33**(26), 1830025 (2018)
67. Rogers, T.C.: Eur. Phys. J. **A52**(6), 153 (2016)
68. Schweitzer, P., Strikman, M., Weiss, C.: JHEP **01**, 163 (2013)
69. Scimemi, I., Vladimirov, A.: Eur. Phys. J. **C78**(2), 89 (2018)
70. She, J., Zhu, J., Ma, B.Q.: Phys. Rev. **D79**, 054008 (2009)